Specific Solvation Interactions of CO_2 on Acetate and Trifluoroacetate Imidazolium Based Ionic Liquids at High Pressures

Pedro J. Carvalho,[†] Víctor H. Álvarez,[‡] Bernd Schröder,[†] Ana M. Gil,[†] Isabel M. Marrucho,[†] Martín Aznar,[‡] Luís M. N. B. F. Santos,[§] and João A. P. Coutinho*,[†]

CICECO, Departamento de Química, Universidade de Aveiro, 3810-193 Aveiro, Portugal, Faculdade de Engenharia Química, Universidade Estadual de Campinas, 13083-970 Campinas, SP, Brasil, Centro de Investigação em Química, Faculdade de Ciências da Universidade do Porto, Universidade do Porto, R. Campo Alegre, 687 4169-007 Porto, Portugal

Received: February 11, 2009; Revised Manuscript Received: March 13, 2009

New classes of acidic or basic ionic liquids (ILs) are gaining special attention, since the efficiency of many processes can be enhanced by the judicious manipulation of these properties. The absorption of sour gases can be enhanced by the basic character of the IL. The fluorination of the cation or the anion can also contribute to enhance the gas solubility. In this work these two characteristics are evaluated through the study of the gas−liquid equilibrium of two ionic liquids based on similar anions, 1-butyl-3-methylimidazolium acetate ([C_4mim][Ac]) and 1-butyl-3-methylimidazolium trifluoroacetate ([C_4mim][TFA]), with carbon dioxide (CO_2) at temperatures up to 363 K and pressures up to 76 MPa. The data reported are shown to be thermodynamically consistent. Henry's constants estimated from the experimental data show the solubility of CO_2 on the [C_4mim][Ac] to be spontaneous unlike in [C_4mim][TFA] due to the differences in solvation enthalpies in these systems. Ab initio calculations were performed on simple intermolecular complexes of CO_2 with acetate and trifluoroacetate using MP2/6-31G(d) and the G3 and G3MP2 theoretical procedures to understand the interactions between CO_2 and the anions. The theoretical study indicates that although both anions exhibit a simultaneous interaction of the two oxygen of the carboxylate group with the CO_2, the acetate acts as a stronger Lewis base than the trifluoroacetate. ^{13}C high-resolution and magic angle spinning (HRMAS) NMR spectra provide further evidence for the acid/base solvation mechanism and the stability of the acetate ion on these systems. Further similarities and differences observed between the two anions in what concerns the solvation of CO_2 are discussed.

Introduction

Ionic liquids (ILs) are a class of *neoteric* organic solvents that have been the object of an unprecedented burst of interest, both from academia and industry, in recent years. The large organic cations and asymmetrical organic or inorganic anions compel these molecules to remain liquid at or near room temperature, while presenting, among other relevant properties, negligible vapor pressures, high thermal stability, large liquidus range, nonflammability, and high solvation capacity.[1−4] The tunable properties of ILs, through an endless combination of cations and anions, allow the design of solvents for the development of more efficient and sustainable processes and products. These compounds' aptness for fine-tuning of their properties cataloged them as *designer solvents*. However, the design of a task-specific compound requires the definition of target properties and of the characteristics that are behind them.

Among the several applications foreseeable for task-specific ionic liquids such as solvents for reactions involving gaseous reactants and products,[5] catalysts for acid-catalyzed organic reactions,[6] and chemical absorption,[7] their use in processes with compressed gases for capture/sequestration of sour gases such as CO_2, H_2S, and SO_2, in refinery, coal combustion, and cleaning of gas streams, is one of the most exciting.

A considerable amount of work, concerning the development of task-specific ionic liquids, has been carried out, addressing essentially the IL cation. Bates el al.[8] reported amino-functionalized ILs, while Yuan et al.[9] and Sun et al.[10] used hydroxyl-functionalized ILs as a novel efficient catalyst for chemical fixation of CO_2. Yu et al.[7] and Huang et al.[5] proposed guanidinium-based ILs, where the electron-donating groups increased the strength of the donor−acceptor interactions on -NH_2 and consequently enhanced the interactions between -NH_2 and CO_2. Li et al.[6] investigated the ability of switching the ILs basicity by repeatedly bubbling CO_2 and N_2, improving efficiency of the processes. Bara et al.[11] synthesized imidazolium-based ILs with one, two, or three oligo(ethylene glycol) substituents that, in spite of presenting CO_2 solubilities similar to that in [$C_n$mim][Tf_2N] analogues, present lower solubilities toward N_2 and CH_4 and therefore enhanced selectivities.

Acidic or basic ILs represent new classes of acids or bases. The study of the acidity/basicity of the ILs is of great importance, since the efficiency of many processes depends on the basicity of the media or can be controlled by it. Crowhurst et al.[12] reported that the hydrogen bond basicities of ILs are controlled by the anion, and the hydrogen bond donating behavior is also dominated by the hydrogen bond basicity of the anions, with a smaller contribution from the hydrogen bond acidity of the cation. Furthermore, for the imide ionic liquids

* To whom correspondence should be addressed. Tel.: +351 234 401 507. Fax: + 351 234 370 084. E-mail: jcoutinho@ua.pt.
[†] Universidade de Aveiro.
[‡] Universidade Estadual de Campinas.
[§] Universidade do Porto.

10.1021/jp901275b CCC: $40.75
Published on Web 04/17/2009

an increase of the hydrogen bond acidity with the cation change was found.[12] Nonetheless, changing to more basic anions leads to a dramatic drop in the acidity. Pennline et al.[13] screened quaternary ammonium polyether ILs as potential solvents for CO_2 capture based in the Pearson's "hard and soft acid−base" principles, where the solvent should possess a Pearson "hard base" allowing a strong affinity toward CO_2. Maginn et al.[14] and Shiflett et al.[15−17] reported on imidazolium-based ionic liquid with the acetate and other carboxylate anions that seem to present an uncharacteristic behavior. The systems with the acetate-based IL present a low vapor pressure for mixtures up to about 20 mol %, indicating that CO_2 could have formed a nonvolatile or very low vapor pressure molecular complex with the ionic liquid. The solvation of CO_2 by these anions is, however, yet poorly understood.

The present study will explore the basicity of the anion as a means to enhance the absorption of sour gases by ionic liquids, along with another strategy to foster the gas solubility in an IL by the fluorination of its alkyl chains.[18,19] In this work the two effects will be compared and evaluated in a wide range of pressures and temperatures aiming at a better understanding of the mechanisms of solvation of CO_2 on ILs with these characteristics. For that purpose the gas−liquid equilibrium (GLE) of the atypical and challenging binary systems, CO_2 + 1-butyl-3-methylimidazolium acetate ([C_4mim][Ac]), and CO_2 + 1-butyl-3-methylimidazolium trifluoroacetate ([C_4mim][TFA]) previously approached only by Shiflett et al.,[15−17] will be here extended to higher pressures, temperatures, and concentrations. The comparison between these two systems will provide not only a better understanding of the anion acid/base interactions with the CO_2 but also the influence of the fluoroalkyl groups in the molecule behavior and consequently, in the CO_2 solubility. A thermodynamic consistency test developed for systems with incomplete *PTxy* data,[20−23] is here used to evaluate the quality of the data reported through its thermodynamic consistency.

There is plenty of evidence in the literature for Lewis acid/Lewis base (A/B) interaction between CO_2 and the carbonyl group.[24−26] Raveendran and Wallen[27] have studied the role of a cooperative C−H···O interaction as an additional stabilizing interaction between the CO_2 and the carbonyl group and their implications for the solvation of CO_2 on these compounds. The CO_2 acts as a LA where the acidic central carbon interacts with charged or uncharged Lewis bases.

To understand the interactions between CO_2 and the [Ac] and [TFA] anions, ab initio calculations were performed on simple intermolecular complexes using MP2/6-31G(d), and the G3 and G3MP2 theoretical procedures. A simultaneous interaction, of the two oxygens of the carboxylate group with the CO_2, is found in both anions, [Ac] and [TFA].

^{13}C high-resolution and magic angle spinning (HRMAS) NMR spectra of the CO_2 + [C_4mim][Ac] are shown to further support the acid/base interaction mechanism behind the solvation of CO_2 at low pressures. They also provide further evidence to the stability of the acetate on these systems.

Experimental Section

Materials. Two ILs based on the 1-butyl-3-methylimidazolium cation, namely, 1-butyl-3-methylimidazolium trifluoroacetate [C_4mim][TFA] and 1-butyl-3-methylimidazolium acetate [C_4mim][Ac], were used on this study. The [C_4mim][TFA] was acquired from Solchemar with mass fraction purities > 99% and bromide impurity mass fraction < 10^{-4}, while the [C_4mim][Ac] was synthesized by means of carbonate-based ionic liquid synthesis (CBILS) of proionic/Sigma-Aldrich.[28] 1-Butyl-3-methylimidazolium hydrogencarbonate (the CBIL precursor as a 50.0% solution in H_2O) was treated with an exact stoichiometric amount of acetic acid (FIXANAL/Riedel-de Haën). After the evolution of CO_2 ceased, water and solvents were removed under vacuum. The purities stated by the supplier and those of the [C_4mim][Ac] IL, were checked by ^{1}H NMR, ^{13}C NMR, and ^{19}F NMR. For the [C_4mim][Ac] the ^{1}H NMR obtained presents the following(chloroform-*d*, δ/ppm relative to TMS): 10.56 (s, 1H), 7.47 (d, 2H), 4.08 (s, 6H).

It is well-established that IL physical properties are influenced by their water content.[29−32] Blanchard et al.[33] reported that even minor amounts of water, dissolved in [C_4mim][PF_6], lead to a reduction of 77% on the CO_2 solubility. More recently, in a systematic study on the influence of water on the solubility of CO_2 for the same compound, Fu et al.[34] reported a less pronounced, <15%, influence. Nonetheless, these reports clearly state the importance of implementing purifying procedures prior to the measurements. Thus, to reduce the content of water and volatile compounds to negligible values, vacuum (0.1 Pa), stirring and moderate temperature (353 K) were applied for a period of at least 48 h prior to the measurements to the ILs. The final water content was determined with a Metrohm 831 Karl Fischer coulometer, indicating a water mass fraction of 495×10^{-6} and 554×10^{-6} for [C_4mim][TFA] and [C_4mim][Ac], respectively.

The CO_2 used was from Air Liquide with a purity of ≥99.998% and H_2O, O_2, C_nH_m, N_2, and H_2 impurity volume fractions lower than 3×10^{-6}, 2×10^{-6}, 2×10^{-6}, 8×10^{-6}, and 0.5×10^{-6}, respectively.

Experimental Measurements. The high-pressure equilibrium cell used in this work is based on the synthetic method and is sketched in Figure 1. The cell is based on the design of Daridon et al.[35−39] and was previously found to be adequate to measure IL systems.[35,39] It consists of a horizontal hollow stainless steel cylinder, closed at one end by a movable piston and at the other end by a sapphire window. This window, along with a second window on the cell wall through which an optical fiber lights the cell chamber, allows the operator to follow the behavior of the sample with pressure and temperature. The orthogonal positioning of the sapphire windows minimizes the parasitic reflections and improves the observation in comparison to axial lighting.

A small magnetic bar placed inside the cell allows the homogenization of the mixture by means of an external magnetic stirrer. The sapphire window on the cell wall limits the minimum internal volume of the cell to 8 cm^3, while the maximum value is set to 30 cm^3. The presence of the magnetic stirrer as well as the cell reduced volume helps to minimize the inertia and temperature gradients within the sample.

The cell is thermostatized by circulating a heat-carrier fluid through three flow lines directly managed into the cell. The heat-carrier fluid is thermoregulated with a temperature stability of ±0.01 K by means of a thermostat bath circulator (Julabo MC). The temperature is measured with a high precision thermometer, Model PN 5207 with an accuracy of 0.01 K connected to a calibrated platinum resistance inserted inside the cell close to the sample. The pressure is measured by a piezoresistive silicon pressure transducer (Kulite HEM 375) fixed directly inside the cell to reduce dead volumes, which was previously calibrated and certified by an independent laboratory with IPAC accreditation, following the EN 837-1 standard and with accuracy better than 0.2%.

A fixed amount of IL was introduced inside the cell; its exact mass was determined by weighting, using a high-weight/high-

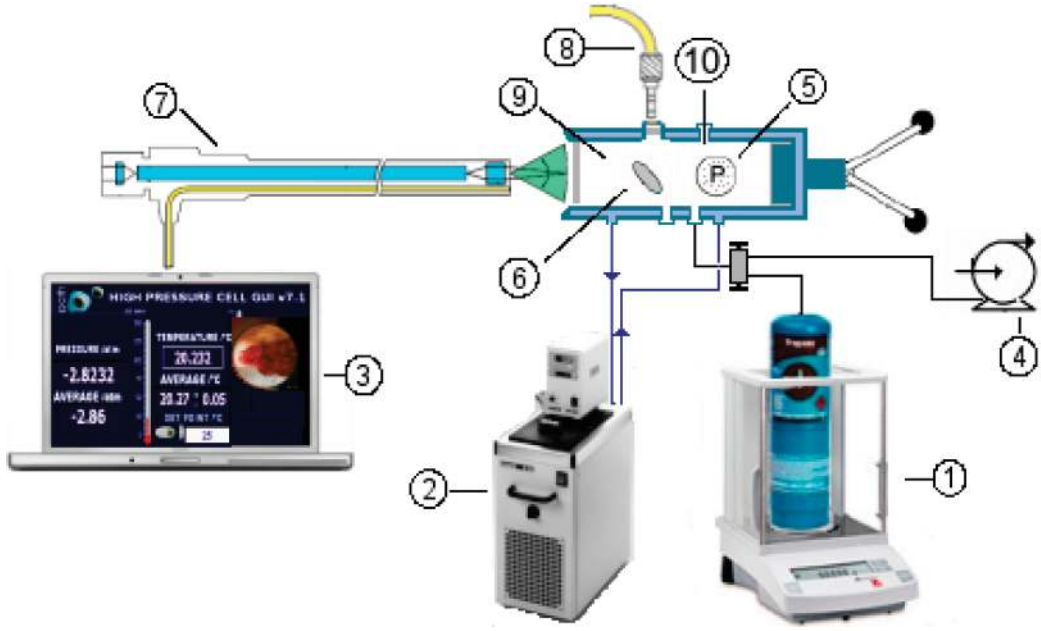

Figure 1. Schematic apparatus: 1, analytical balance (Sartorius LA200P); 2, thermostatized bath circulator (Julabo MC); 3, computer for data and video acquisition; 4, vacuum pump (Edwards RV3); 5, piezoresistive pressure transducer (Kulite HEM 375); 6, magnetic bar; 7, endoscope plus a video camera; 8, light source with optical fiber cable; 9, high-pressure variable-volume cell; 10, temperature probe (K type thermocouple).

precision balance with an accuracy of 1 mg (Sartorius LA2000P). To avoid any interference of atmospheric gases during the manipulation, after placing the IL inside the cell, this was kept under vacuum overnight, while stirring and heating at 353 K.

The CO_2 was introduced under pressure from an aluminum reservoir tank. Its quantity was measured on the precision balance and introduced into the measuring cell by means of a flexible high-pressure capillary.

After preparation of a mixture of known composition, it was allowed to reach the desired temperature at low pressure; the pressure was then slowly increased at constant temperature until the system becomes monophasic. The pressure at which the last bubble disappears represents the equilibrium pressure for the fixed temperature.

The purity of the IL is checked again by NMR at the end of the study to confirm that no degradation of the IL takes place during the measurements. The ^1H, ^{13}C, and ^{19}F NMRs spectra were recorded using a Bruker Avance 300 at 300.13 MHz using deuterated water (D_2O) and/or deuterated chloroform ($CDCl_3$) as solvents (below the IL saturation limit and low enough to ensure complete dissociation in aqueous solution).

^{13}C HRMAS spectra were recorded on a Bruker Avance DRX-500 spectrometer resonating at 125.8 MHz for carbon and using a HRMAS 4 mm double-bearing probe. The use of HRMAS technology allows higher resolution to be obtained for viscous liquids such as the ILs hereby studied. MAS rotors with a fixed bottom spacer and a sealable top spacer were employed, accommodating a total of 60 μL of sample (50 μL of ionic liquid and 10 μL of 0.75% 3-(trimethylsilyl)propionate sodium salt (TSP) D_2O solution for chemical shift reference and lock purposes). Spectra were acquired at a 4 kHz spinning rate, with a 90° pulse of 5.3 μs, a 2 s recycle delay, and 128 or 256 scans.

Thermodynamic Modeling and Consistency

Valderrama and Álvarez[21−23] developed a thermodynamic consistency test for systems with incomplete *PTxy* data, cataloging them as thermodynamic consistent (TC), thermodynamic inconsistent (TI), or not fully consistent (NFC). As in previous works[16,23,38] we have applied an extension of this approach to CO_2 + IL systems using a method based on the Gibbs−Duhem equation, using the Peng−Robinson equation of state (EoS),[40] with the Wong−Sandler mixing rule.[41] A detailed description of that approach can be found in the Supporting Information. The equation of state was used to estimate the Henry's constants for the systems studied.[16]

Results and Discussion

Experimental Data. High-pressure gas−liquid data for mixtures of CO_2 and ILs are scarce, and important discrepancies among data from different authors[19,42,43] can be found in the literature.

The solubility of carbon dioxide in the ILs studied in this work was measured for mole fractions from 0.2 to 0.8, in the temperature range from 293 to 363 K and pressures from 0.2 to 76 MPa, as reported in Tables 1 and 2 and depicted in Figure 2. The shape of the phase diagrams obtained for these systems is analogous to what was previously reported to binary mixtures of CO_2 and ionic liquids. At low CO_2 concentrations, the pressure increase with the CO_2 content is almost linear, while for CO_2 mole fractions higher than 0.4 for [C_4mim][Ac] and 0.55 for [C_4mim][TFA] a dramatic increase in pressure with concentration is observed. At temperatures below the CO_2 critical temperature a two-phase region is observed above these concentrations. The most surprising feature observed on these systems is the very large solubility of CO_2 in [C_4mim][Ac] up to a mole fraction of 0.3. This IL seems to be able to dissolve a very large amount of carbon dioxide at low pressure. This was also observed by Shifflet et al.[15−17] In spite of this larger solubility at low pressures, as the CO_2 concentration increases, its solubility in [C_4mim][Ac] becomes inferior to the solubility in [C_4mim][TFA] as observed in Figure 3.

The results of the application of the thermodynamic consistency test to the binary systems containing ionic liquids is presented in Table 3 for the thermodynamically consistent data, and in the Supporting Information, for all the experimental data. In this table, NP is the number of data points, *T* is the

TABLE 1: Bubble Point Data of the System CO_2 (1) + [C_4mim][Ac]

x_1	T/K	p/MPa	x_1	T/K	p/MPa
0.201	323.05	0.230	0.402	323.57	5.272
0.201	333.07	0.355	0.402	333.35	6.580
0.201	343.18	0.652	0.402	343.16	8.060
0.201	353.10	0.971	0.402	353.24	9.850
0.251	313.09	0.498	0.450	313.09	5.730
0.251	322.96	0.830	0.450	323.00	7.394
0.251	333.30	1.275	0.450	333.27	9.564
0.251	343.05	1.695	0.450	343.06	12.188
0.251	353.20	2.235	0.450	353.18	15.281
0.300	313.04	1.398	0.500	322.98	13.478
0.300	323.22	1.923	0.500	333.06	18.051
0.300	333.33	2.515	0.500	343.10	22.985
0.300	343.10	3.205	0.500	353.13	28.055
0.300	352.98	3.980	0.550	313.31	27.965
0.351	313.04	2.589	0.550	323.40	34.865
0.351	322.83	3.360	0.550	333.37	41.807
0.351	333.42	4.288	0.550	343.25	48.107
0.351	343.22	5.265	0.550	353.05	53.904
0.351	353.22	6.430	0.599	313.10	67.371
0.402	313.07	4.090	0.599	323.09	75.526

TABLE 2: Bubble Point Data of the System CO_2 (1) + [C_4mim][TFA]

x_1	T/K	p/MPa	x_1	T/K	p/MPa
0.225	293.43	0.979	0.502	313.18	5.860
0.225	303.22	1.338	0.502	323.49	7.413
0.225	313.20	1.706	0.502	333.35	9.135
0.225	323.11	2.146	0.502	343.07	11.151
0.225	333.35	2.587	0.502	353.03	13.225
0.225	343.23	3.105	0.502	363.03	15.498
0.225	353.08	3.612	0.601	293.44	7.936
0.225	363.04	4.165	0.601	303.21	13.268
0.300	293.25	1.540	0.601	313.21	18.548
0.300	303.30	2.056	0.601	323.21	22.835
0.300	313.15	2.619	0.601	333.09	28.263
0.300	323.08	3.160	0.601	343.14	32.589
0.300	333.06	3.912	0.601	353.10	36.545
0.300	343.15	4.726	0.601	363.12	42.075
0.300	353.13	5.559	0.650	293.46	26.422
0.300	363.18	6.416	0.650	303.35	32.581
0.401	293.52	2.419	0.650	313.17	37.835
0.401	303.23	3.108	0.650	323.04	43.392
0.401	313.14	3.959	0.650	333.25	48.458
0.401	323.04	4.840	0.650	343.06	52.947
0.401	333.08	5.996	0.650	353.11	56.890
0.401	343.02	6.957	0.650	363.10	62.989
0.401	353.07	8.144	0.679	293.59	43.625
0.401	363.07	9.337	0.679	303.34	50.189
0.502	293.61	3.513	0.679	313.08	55.966
0.502	303.40	4.611	0.679	323.08	62.473

temperature, and k_{12}, α_{12}, $g_{12}-g_{22}$ and $g_{21}-g_{11}$ are the interaction parameters of the model, where 1 stands for the CO_2 and 2 for the ionic liquid. This table is divided into sections for each system studied. The CO_2 + [C_4mim][Ac] system determined by Shifflet et al.[15] was also investigated. The parameters used in the thermodynamic model are reported in Table 4. The consistency test shows that, in general, the data measured in this work are thermodynamically consistent with the exception, in a few cases, of the mixtures richer in CO_2. The results obtained denote larger deviations in individual areas for the CO_2 + [C_4mim][Ac] system for $x_1 > 0.5$ isopleths and for the CO_2 + [C_4mim][TFA] system for the $x_1 > 0.65$ isopleths leading to not fully consistent isotherms. However, these data points at higher CO_2 concentrations must be considered with care, since they present a more complex phase behavior which could be the cause for the apparent inconsistencies. The data for the CO_2 + [C_4mim][Ac] system here reported present a thermodynamic coherence superior to the data previously reported by Shifflet et al.,[15] in particular at lower and higher temperatures for which the data present deviations larger than the established limit for the values of $\%\Delta p_i$ and thereafter, the test could not be applied, denoting inaccuracies in the experimental data measurements.

As depicted in Figure 4, the equation of state used provides a good description of the experimental data.

Henry's Constants. Henry's law relates the fugacity of a gas dissolved in a liquid with its concentration and can be described as

$$H_{12}(T,P) = \lim_{x_1 \to 0}\left(\frac{f_i^L}{x_1}\right) \tag{1}$$

where $H_{12}(T,P)$ is the Henry's constant, x_1 is the mole fraction of gas dissolved in the liquid phase, and f_1^L is the fugacity of gas in the liquid phase. As shown, eq 1 is only rigorously valid in the diluted region limit. Given the good description of the experimental data provided by the equation of state used, the Henry constants for the CO_2 in the ILs studied in this work were estimated by extrapolating the equation of state description of the experimental data to the dilute region.[16] Although this approach introduces some uncertainty on the estimated Henry's constants, they are different enough to allow a discussion of the interactions between the CO_2 and the ionic liquid based on these values. The estimated Henry's constants are reported in Table 3. The results indicate that the Henry's constant decreases slightly (i.e., CO_2 solubility increases) as the temperature decreases. Nonetheless, Henry's constant for the [C_4mim][TFA] presents a larger temperature dependence than the one of [C_4mim][Ac].

The results for the Henry's constant of CO_2 in [C_4mim][Ac] and CO_2 in [C_4mim][TFA] were correlated as a function of temperature by an empirical equation of the type

$$\ln(H_{12}) = A\left(\frac{1}{T}\right) + B \tag{2}$$

where coefficients A and B obtained are listed in Table 5, together with the Henry's constant average absolute deviations, $|\Delta H_{12}|$, obtained for each ionic liquid.

The effect of temperature on the CO_2 solubility can be related to the Gibbs energy of solvation, the partial molar entropy, and the partial molar enthalpy of solvation[44] that can be calculated from an appropriate correlation of Henry's constant:

$$\Delta_{solv}G^\circ = RT(\ln(H_{12}))_p \tag{3}$$

$$\Delta_{solv}H^\circ = -T^2\left(\frac{\partial \Delta_{solv}G^\circ}{\partial T}\right)_T = -RT^2\left(\frac{\partial \ln H_{12}}{\partial T}\right)_p \tag{4}$$

$$\Delta_{solv}S^\circ = \frac{\Delta_{solv}H^\circ - \Delta_{solv}G^\circ}{T} = -RT\left(\frac{\partial \ln H_{12}}{\partial T}\right)_p - R\ln(H_{12})_p \tag{5}$$

The partial molar enthalpy of gas solvation gives an indication of the strength of interactions between the gas and IL, while the partial molar entropy illustrates the amount of ordering present in the gas/IL mixture.

The results in Table 5 show that the partial molar entropies in both fluids are essentially identical, indicating a similar structural solvation interaction. The partial molar enthalpy of solvation of the CO_2 in [C_4mim][Ac] is lower than in [C_4mim][TFA], indicating a stronger interaction between the

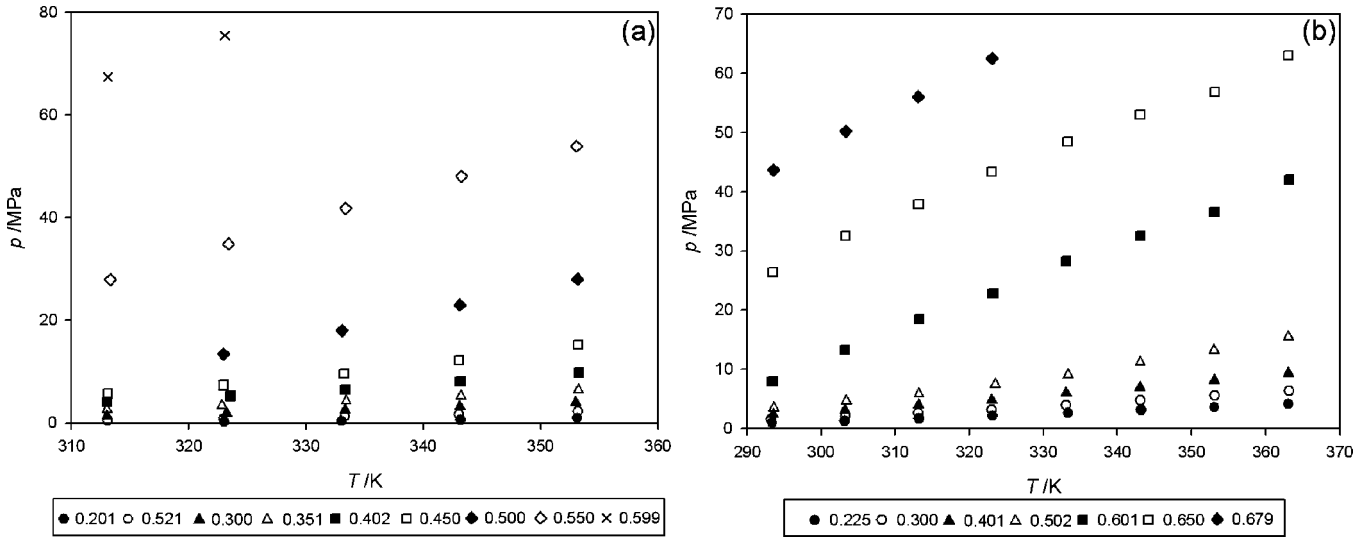

Figure 2. Pressure−temperature diagram of the binary systems (a) CO_2 + [C_4mim][Ac] and (b) CO_2 + [C_4mim][TFA].

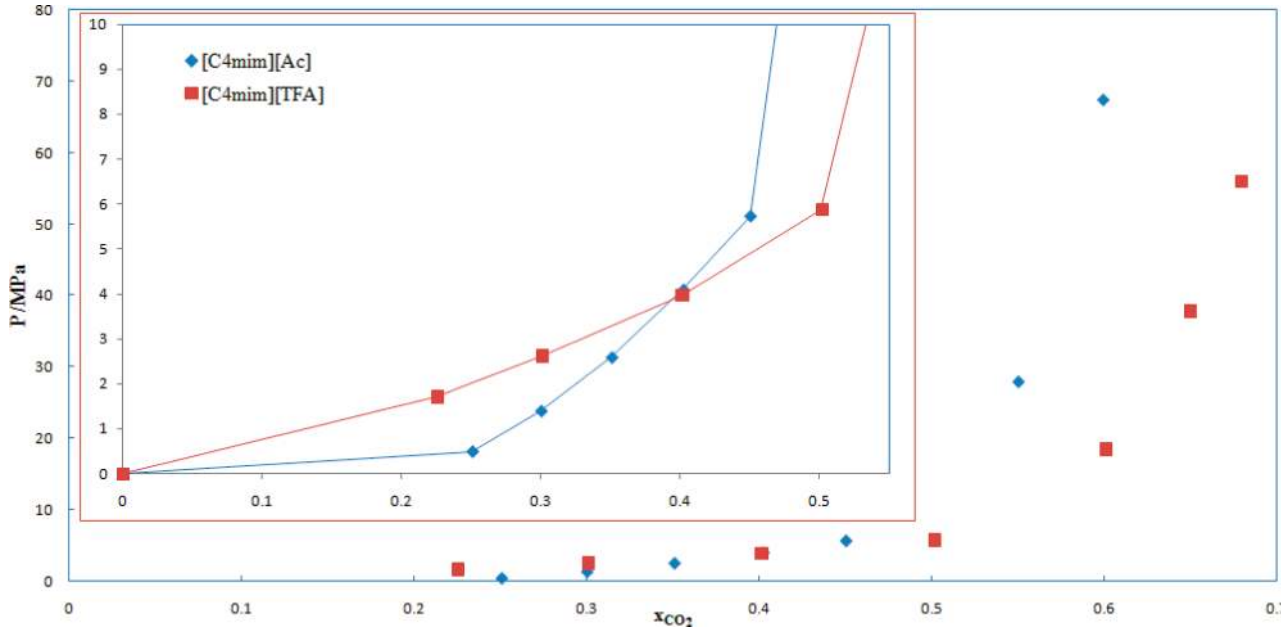

Figure 3. Pressure−composition diagram of the binary systems CO_2 + [C_4mim][Ac] and CO_2 + [C_4mim][TFA] at 313 K.

CO_2 and the [C_4mim][Ac] when compared with the [C_4mim][TFA]. The differences between the enthalpies and entropies of solvation contribution observed make the solubility of CO_2 in [C_4mim][Ac] spontaneous, unlike for [C_4mim][TFA], which explains the large solubility observed at low pressures.

To obtain further information about the interaction CO_2/[C_4mim][Ac], which seems to be responsible for the enhanced solubility of CO_2 in this IL at low pressures, ^{13}C HRMAS NMR spectra of the pure and CO_2-saturated IL at atmospheric pressure were acquired and reported in Figure 5. The comparison between the two spectra shows an important downfield shift of the carboxylate carbon (11) (from 179 to 183 ppm) due to the presence of CO_2 and indicating the Lewis acid/base interaction to be responsible for the enhanced solubility of CO_2 in this solvent. The upfield shift in carbon (12), the other anion carbon, results also from this acid/base interaction with CO_2. The other major difference observed on these spectra is related to the cation carbon (2), which is connected to an acid hydrogen. In the absence of CO_2 (Figure 5a), this resonance is significantly broadened and so are, to a lesser extent, ring resonances C(4) and C(5). This is expected due the proximity to the quadrupolar nuclei of the neighboring ^{14}N atoms, in case molecular motion is relatively slow and unable to average out $^{13}C/^{14}N$ interactions. The introduction of CO_2 in the system will shift the interaction of the acetate from the imidazolium ring, and particularly C(2), toward the gas, increasing the mobility of the imidazolium ring with a noticeable effect on the peaks of the carbon at the imidazolium ring, most spectacularly C(2). Interestingly, in both systems resonances C(6) and C(10) are also broadened due to nitrogen proximity. These spectra also confirm that, even in the presence of CO_2, there is no formation of acetic acid in the system as suggested by some authors.[14,15] The fact that a CO_2 peak is not observed (possibly at about 120−130 ppm) can only be attributed to the high mobility of this molecule in solution. Its strong interaction with the acetate does not bind it to the carboxylate group but instead the CO_2 must be quickly changing among neighbor carboxylates.

Solubility measurements,[43,45] spectroscopic studies,[46] and molecular simulations[45] indicated that CO_2 solubility in ILs depends primarily on the strength of interaction of the CO_2 with

TABLE 3: Estimated Interaction Parameters, for the Thermodynamically Consistent Data, and Henry Constant Predicted for the CO_2 (1) + ILs (2) Systems at Different Temperatures

ref	NP	T/K	k_{ij}	α_{12}	$g_{12}-g_{22}$/(J /mol)	$g_{21}-g_{11}$/(J /mol)	$\lvert\Delta p\rvert$/%	$\lvert\Delta A\rvert$/%	H/MPa
					CO_2 + [C_4mim][Ac]				
15	8	298.10	−0.6470	0.2166	−32855.6133	5999.5654	2.5	6.1	
	7	323.10	1.0000	0.3244	−11206.7412	2763.3943	3.4	7.3	
this work	5	313.10	−0.0146	0.2979	−29707.8203	7932.1289	1.3	3.8	0.056
	7	323.09	−0.3497	0.2482	−50410.7500	−1595.7640	1.0	4.6	0.086
	7	333.00	0.2981	0.3177	−40720.8945	−2724.8025	2.6	9.4	0.121
	7	343.00	−0.8572	0.3043	−44254.0312	89950.4766	4.2	10.8	0.137
	6	348.00	0.7969	0.4229	−32920.5625	−3534.8833	1.2	2.7	0.203
	6	352.98	0.9949	0.4392	−33570.1133	−4218.7607	0.8	3.7	0.253
					CO_2 + [C_4mim][TFA]				
this work	5	294.00	0.2188	0.2045	34112.2930	−2444.4580	5.8	4.3	3.40
	5	298.00	0.2236	0.2059	34037.5859	−2354.5664	6.2	4.7	3.85
	5	303.00	0.2422	0.2027	34804.6875	−2620.2393	3.1	7.1	4.03
	4	313.00	0.0625	0.2132	35599.7812	−1764.0344	0.6	4.2	5.93
	4	323.00	0.2745	0.2497	33887.6523	−1097.2380	0.8	4.4	7.45
	5	333.00	−0.0063	0.2001	42388.7930	−1258.0310	0.7	15.3	8.97
	5	343.00	0.0801	0.2000	45219.8125	−781.5312	1.2	11.7	11.74
	5	348.00	−0.0001	0.2008	46516.1133	−791.0156	1.5	9.3	11.94
	5	353.00	0.1250	0.2006	47268.5469	−702.7494	1.9	12.5	13.50
	4	363.00	0.1601	0.2026	46758.0273	−1230.8120	6.0	4.4	13.57

TABLE 4: Properties of the Substances Used in the Modeling

compound	T_c/K	p_c /MPa	ω
CO_2	304.21[a]	7.38[a]	0.2236[a]
[C_4mim][TFA]	826.72[b]	2.09[b]	0.6891[b]
[C_4mim][Ac]	847.31[b]	2.44[b]	0.6681[b]

[a] Reference 57. [b] Calculated with ref 23.

the anion. Furthermore, Crowhurst et al.[12] reported that in terms of solvation the ionic liquid hydrogen bond donor behavior was dominated by the hydrogen bond basicity of the anions, with a low contribution from the hydrogen bond acidity of the cation. Thus, the presence of fluoroalkyl groups in the basic trifluoroacetate anion based ILs[47] makes them "CO_2-philic", meaning that they present higher CO_2 solubilities than other ILs, resulting in lower equilibrium pressures. This behavior, not yet fully understood, seems to be related to the interaction between the negative fluorine atoms and the positive charge on the carbon of the CO_2 molecule.[19,48−51] Anderson et al.[52] suggests that the Tf_2N anion is the anion displaying the most significant influence in the hydrogen bond donor ability of the IL. In fact, Anderson's statement reflects well the behavior of the [C_4mim][Tf_2N] and [C_4mim][TFA] ILs, since both present higher solubility, than other ILs, for a wider range of CO_2 mole fractions.[39,53]

The comparison between the solubilities of CO_2 in [C_4mim][Ac] and [C_4mim][TFA] reveals a curious behavior. For low CO_2 molar fractions (<30%) the [C_4mim][Ac] presents higher CO_2 solubility than any IL previously studied[15] but, as the CO_2 molar fraction increases, the solubility in [C_4mim][Ac] quickly drops below the solubility in [C_4mim][TFA] as shown in Figure 3. This behavior could be explained by a chemisorption taking place in [C_4mim][Ac] at low CO_2 pressure, but as the chemical solvation sites become saturated and the physisorption dominates, the solvation capacity of the fluorinated acetate becomes dominant. The fluorination of the acetate seems however to reduce its chemical solvation capacity. For a deeper understanding of these interactions we resorted to ab inito calculations to analyze the interactions between the fluorinated and non-fluorinated acetate and the CO_2.

Ab Initio Calculations. Ab initio calculations on the CO_2/[Ac] and CO_2/[TFA] interactions were performed using the Gaussian 03 program.[54] Geometry optimizations were performed at the second-order Møller−Plesset (MP2) level using the 6-31+G(d) basis set to include the effects of electron correlation. The vibrational frequencies were also calculated to confirm that the structures were at the real potential energy minimum. The optimized geometries are shown in Figures 6 and 7 for the CO_2 complex with the acetate and trifluoroacetate, respectively. The CO_2 is interacting as Lewis acid with the acetate group, which acts as Lewis base. The CO_2 molecule is significantly distorted from linearity. The shorter C(carboxylate) to C(CO_2) distance and the larger CO_2 distortion angle in the CO_2 complex with the acetate is a structural indication that the CO_2/[Ac] interaction is stronger than CO_2/[TFA]

Conformation "B", depicted in Figure 8, represents the complex formation of the CO_2 with the oxygen of the carboxylate that was found to have a local energy minimum with a MP2/6-31+G(d).

The Gaussian-3 (G3)[55] and (G3MP2)[56] theoretical procedures were used to evaluate the interaction enthalpies of the complexes between the acetate Lewis base (B) and the CO_2 Lewis acid (A) according the following equation:

$$\Delta H = H_{AB} - (H_A + H_B) \quad (6)$$

where H_{AB} is the G3 or G3MP2 enthalpy of the CO_2 complex with acetate or trifluoroacetate and the H_A and H_B represent the G3 or G3MP2 enthalpies of the monomers. Gaussian-3 (G3) theory is based on the 6-31G(d,p) basis set and several basis extensions, including the G3 large basis set. Geometries are calculated at the MP2(full)/6-31G(d) level, and scaled (0.8929) HF/6-31G(d) zero point energies (ZPEs) are included in the final energies. Treatment of electron correlation is done by Møller−Plesset (MP) perturbation theory and quadratic configuration interaction, and the final energies are effectively performed at the QCISD(T)/G3 large level. Gaussian-3 (G3MP2) theory represents a simplification of the G3 theory with a reduced MP order, thus eliminating the MP4 calculation.

The enthalpic interactions were also evaluated directly using the MP2/6-31+G(d) energies. ZPEs and the enthalpic correction to 298 K were included in the interaction using the MP2 frequencies scaled by 0.95 for the calculation of ZPEs and the enthalpies correction to 298 K. The basis set superposition errors (BSSE) for the MP2/6-31+G(d) interaction was also evaluated

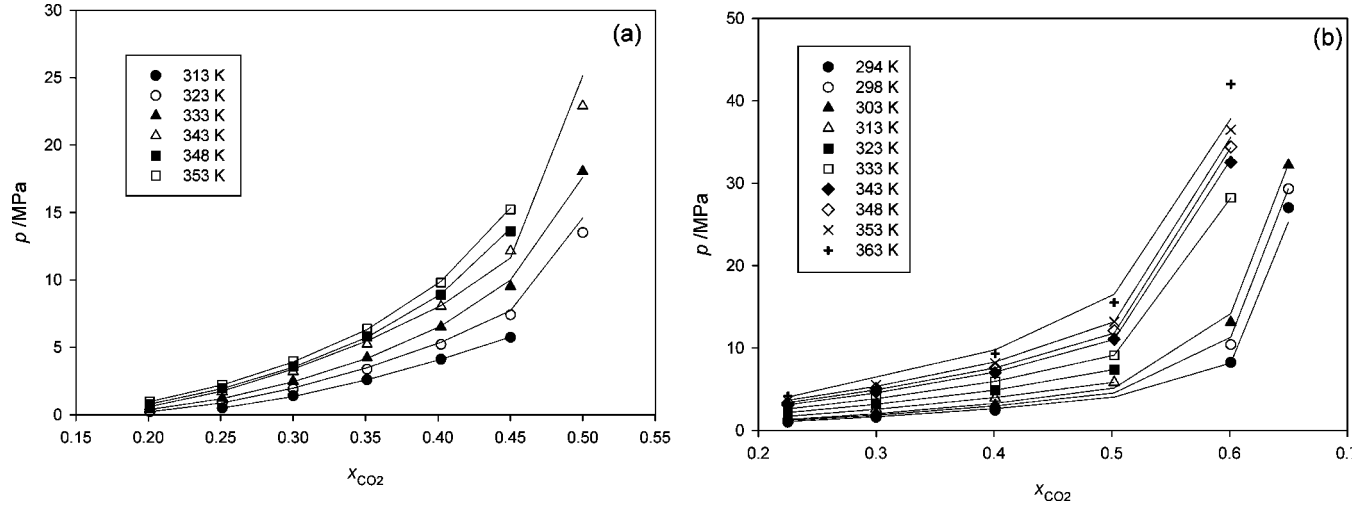

Figure 4. *PTx* diagram and modeling for the systems CO_2 + [C_4mim][Ac] (a) and CO_2 + [C_4mim][TFA] (b). The solid lines represent the calculations from PR-WS/NRTL EoS.

TABLE 5: Coefficients *A* and *B*, Partial Molar Enthalpy, and Partial Molar Entropy Obtained for CO_2 (1) + ILs (2)

ionic liquid	*A*/K	*B*	$\lvert\Delta H_{12}\rvert$/%	$\Delta_{sol}H^{\circ a}$/(kJ mol^{-1})	$\Delta_{sol}S^{\circ\,b}$/(J K^{-1} mol^{-1})	$-T\lvert\Delta_{sol}S^{\circ}_{T=298K}{}^{b}$/(kJ mol^{-1})
[C_4mim][Ac]	−3892 ± 365	11.84 ± 1.09	0.45	−32.4 ± 3.0	−98.5± 9.1	29.4 ± 2.7
[C_4mim][TFA]	−2325 ± 106	11.44 ± 0.33	0.22	−19.3 ± 0.9	−95.2± 2.7	28.4 ± 0.8

[a] Standard enthalpy. [b] Standard (P_0 = 0.1 MPa) molar entropy.

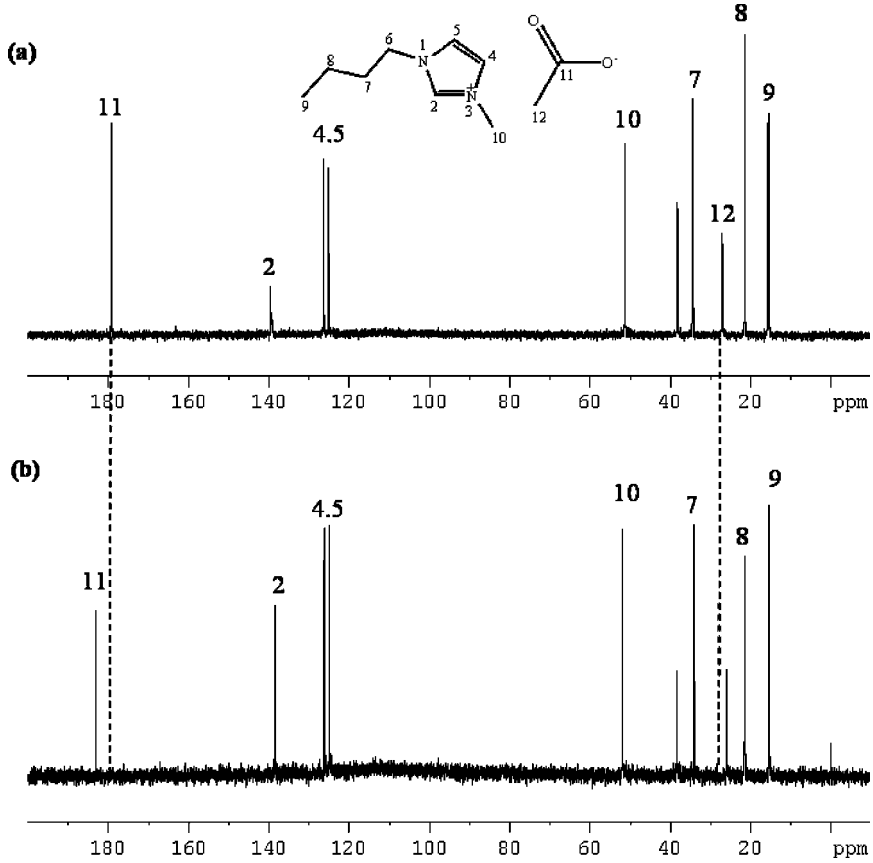

Figure 5. ^{13}C HRMAS NMR spectra for pure [C_4mim][Ac], 128 scans (a), and [C_4mim][Ac] saturated with CO_2, 256 scans (b).

and found to be negligible, taking into account the large energy interaction. The binding enthalpies at the different levels of theory are listed in Table 6. It is interesting to observe that the difference between the enthalpic interactions (acetate and trifluoroacetate) obtained by ab initio in gas phase (7−10 kJ mol^{-1}) present a good agreement with the experimental difference between the enthalpy of solvation of the CO_2 in the [C_4mim][Ac] and in [C_4mim][TFA] (13.1 ± 3.1 kJ mol^{-1}).

The calculated interactions support the idea of a chemisorption of CO_2 in [C_4mim][Ac] but seem to fail in explaining the low, and nonspontaneous nature, of CO_2 solubility in [C_4mim][TFA] as both interactions seem to be similar with a difference of just

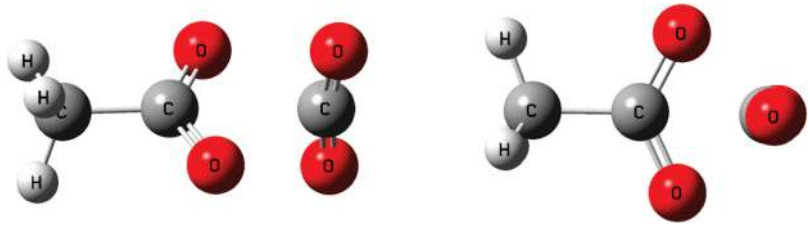

Figure 6. Geometry optimizations of the CO_2−acetate complex (conformation A) at MP2/6-31+G(d) level of theory: carbon to carbon distance C(carboxylate)−C(CO_2), 2.963 Å; CO_2, O−C−O angle, 169.0°.

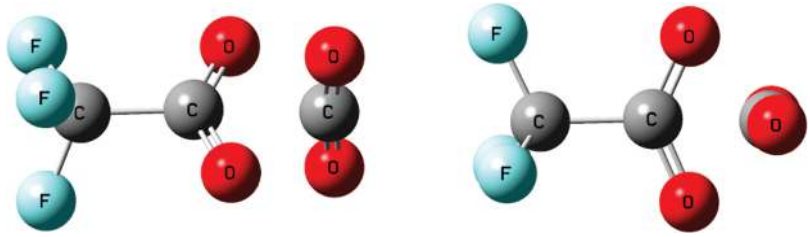

Figure 7. Geometry optimization of the CO_2−trifluoroacetate complex at the MP2/6-31+G(d) level of theory: carbon to carbon distance C(carboxylate)−C(CO_2), 3.059 Å; CO_2, O−C−O angle, 172.9°.

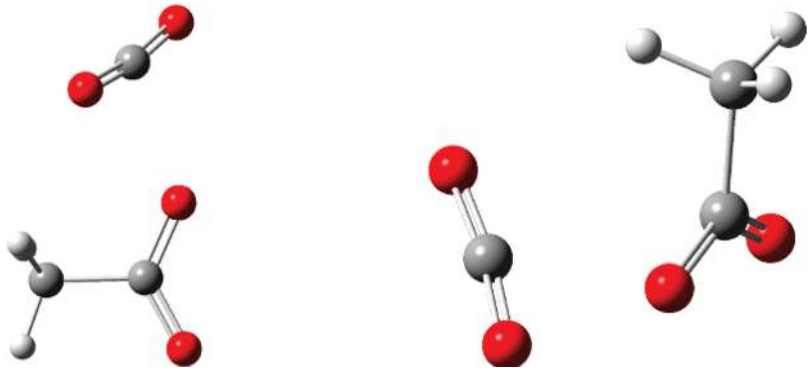

Figure 8. Geometry optimization of the CO_2−acetate complex (conformation B) at the MP2/6-31+G(d) level of theory: carbon to carbon distance O(carboxylate)−C(CO_2), 2.466 Å; CO_2, O−C−O angle, 169.5°.

TABLE 6: Enthalpies of Complex Formation between the Acetate/Trifluoroacetate with the CO_2 in Gas Phase Derived by ab Initio Calculation at Different Levels of Theory (Values in kilojoules per mole)

	ΔH(Ac:CO_2) acetate···CO_2	ΔH(TFA:CO_2) trifluoroacetate···CO_2	diff [b]
Gaussian G3 (conformation "A")	− 41.4	− 33.7	+ 7.7
Gaussian G3(MP2) (conformation "A")	− 39.5	− 32.2	+ 7.3
MP2/6-31+G(d) [a] (conformation "A")	− 42.0	− 31.8	+ 10.2
MP2/6-31+G(d) [a] (conformation "B")	− 29.7		

[a] Zero point energies and enthalpy correction were performed using the values of harmonic frequencies scaled by 0.95. [b] Diff = ΔH(TFA:CO_2) − ΔH(Ac:CO_2).

13 kJ mol^{-1} between the two. Yet this small difference does make all the difference and is indeed enough to explain the differences observed between the two ILs. Since, as shown before, the entropies of solvation are identical in the two ionic liquids, the differences in the Gibbs energy of solvation arise essentially from the differences in the enthalpies of solvation. If eq 3 is used to estimate the differences in the Gibbs energies of solvation between the two fluids in the temperature range of 313−353 K, these values range between 11.6 and 12.1 kJ mol^{-1}. The differences in solubility between the two fluids result essentially from their solvation enthalpy differences and a value of 11−12 kJ mol^{-1} is enough to explain the observed solubility difference. The "chemisorption" observed is nothing more than the expression of the spontaneous solubility of CO_2 on the ionic liquid due to an enthalpy of solvation larger than the corresponding entropy of solvation. We postulate that all ionic liquids with an enthalpy of solvation contribution superior to their entropy of solvation contribution to the Gibbs free energy of solvation, and thus to the solubility, will present a behavior similar to what is presented by [C_4mim][Ac], while the others will behave as [C_4mim][TFA]. This could explain the differences observed between ionic liquids with carboxylate anions studied by Yokozeki et al.,[16] where some do have a "chemisorption-like" behavior while others do not. More studies are however required to provide support for this hypothesis.

Conclusions

Gas solubility of CO_2 in two ionic liquids, namely, 1-butyl-3-methylimidazolium acetate and 1-butyl-3-methylimidazolium trifluoroacetate, has been investigated in a wide range of temperatures, pressures and CO_2 mole fractions, aiming at understanding the effect of the basicity and the fluorination of the anion on the gas solubility in the ionic liquids.

The two systems studied present interesting contrasting behaviors. The binary system 1-butyl-3-methylimidazolium acetate + CO_2 at low pressures presents a high CO_2 solubility, larger than those observed for the other ILs at these pressures, but as the CO_2 molar fraction increases, the solubility decreases exponentially and the solubilities become more important on [C_4mim][TFA] at high pressures.

The data are shown to be thermodynamically consistent, and the Peng−Robinson EoS with the Wong−Sandler/NRTL mixing rule allows a good description of the experimental data and the estimation of the Henry constants for these systems. The partial Gibbs energy, enthalpies, and entropies of solvation estimated from the Henry's constants show the solubility of CO_2 in [C_4mim][Ac] to be spontaneous at the standard pressure (0.1 MPa), while the entropies of solvation in the two systems are essentially identical, making the solubility on these systems controlled by the solvation enthalpies.

^{13}C HRMAS NMR spectra and ab initio calculations indicate that the preferential interaction of the CO_2 with [C_4mim][Ac] results from an acid/base interaction between the carboxylate and the acid carbon in the CO_2 molecule. A good agreement between the measured and calculated differences in the interactions between the CO_2 and the anion in the two systems were obtained, and it is shown that, in the diluted region, a difference in the order of 10 kJ mol^{-1} in the interaction energy is enough to explain the solubility differences observed between the two systems.

Acknowledgment. This work was supported by Fundação para a Ciência e a Tecnologia (Project POCI/EQU/58152/2004). P.J.C. and B.S. acknowledge the financial support from Fundação para a Ciência e a Tecnologia through, respectively, their Ph.D. (Grant SFRH/BD/41562/2007) and postdoctoral scholarships (Grant SFRH/BPD/38637/2007). We acknowledge FAPESP (Fundação de Amparo à Pesquisa do Estado de São Paulo), Process No. 2006/03711-1. We are also grateful to Catarina M. S. S. Neves and Prof. Artur M. Silva for the help with the NMR spectra.

Supporting Information Available: Text describing the thermodynamic modeling and consistency with supporting references and tables listing consistency test results, interpolated VLE data, and detailed results of the studied systems. This material is available free of charge via the Internet at http://pubs.acs.org.

References and Notes

(1) Rogers, R. D.; Seddon, K. R. *Science* **2003**, *302*, 792–793.
(2) Marsh, K. N.; Boxall, J. A.; Lichtenthaler, R. *Fluid Phase Equilib.* **2004**, *219*, 93–98.
(3) Chiappe, C.; Pieraccini, D. *J. Phys. Org. Chem.* **2005**, *18*, 275–297.
(4) Earle, M. J.; Esperanca, J. M. S. S.; Gilea, M. A.; Canongia Lopes, J. N.; Rebelo, L. P. N.; Magee, J. W.; Seddon, K. R.; Widegren, J. A. *Nature (London)* **2006**, *439*, 831–834.
(5) Huang, J.; Riisager, A.; Berg, R. W.; Fehrmann, R. *J. Mol. Catal. A: Chem.* **2008**, *279*, 170–176.
(6) Li, W.; Zhang, Z.; Han, B.; Hu, S.; Song, J.; Xie, Y.; Zhou, X. *Green Chem.* **2008**, *10*, 1142–1145.
(7) Yu, G.; Zhang, S.; Yao, X.; Zhang, J.; Dong, K.; Dai, W.; Mori, R. *Ind. Eng. Chem. Res.* **2006**, *45*, 2875–2880.
(8) Bates, E.; Mayton, R.; Ntai, I.; Davis, J. *J. Am. Chem. Soc.* **2002**, *124*, 926–927.
(9) Yuan, X.; Zhang, S.; Liu, J.; Lu, X. *Fluid Phase Equilib.* **2007**, *257*, 195–200.
(10) Sun, J.; Zhang, S.; Cheng, W.; Ren, J. *Tetrahedron Lett.* **2008**, *49*, 3588–3591.
(11) Bara, J. E.; Gabriel, C. J.; Lessmann, S.; Carlisle, T. K.; Finotello, A.; Gin, D. L.; Noble, R. D. *Ind. Eng. Chem. Res.* **2007**, *46*, 5380–5386.
(12) Crowhurst, L.; Mawdsley, P. R.; Perez-Arlandis, J. M.; Salter, P. A.; Welton, T. *Phys. Chem. Chem. Phys.* **2003**, *5*, 2790–2794.
(13) Pennline, H. W.; Luebke, D. R.; Jones, K. L.; Myers, C. R.; Morsi, B. I.; Heintz, Y. J.; Ilconich, J. B. *Fuel Process. Technol.* **2008**, *89*, 897–907.
(14) Maginn, E. J. *Quarterly Technical Report to DOE*, DOE Award No. DE-FG26-04NT42122, May 31, 2005.
(15) Shiflett, M. B.; Kasprzak, D. J.; Junk, C. P.; Yokozeki, A. *J. Chem. Thermodyn.* **2008**, *40*, 25–31.
(16) Yokozeki, A.; Shiflett, M. B.; Junk, C. P.; Grieco, L. M.; Foo, T. *J. Phys. Chem. B* **2008**, *112*, 16654–16663.
(17) Shiflett, M. B.; Yokozeki, A. *J. Chem. Eng. Data* **2009**, *54*, 108–114.
(18) Muldoon, M.; Aki, S.; Anderson, J.; Dixon, J.; Brennecke, J. *J. Phys. Chem. B* **2007**, *111*, 9001–9009.
(19) Aki, S. N. V. K.; Mellein, B. R.; Saurer, E. M.; Brennecke, J. F. *J. Phys. Chem. B* **2004**, *108*, 20355–20365.
(20) Alvarez, V. H.; Aznar, M. *J. Chin. Inst. Chem. Eng.* **2008**, *39*, 353–360.
(21) Valderrama, J. O.; Àlvarez, V. H. *Fluid Phase Equilib.* **2004**, *226*, 149–159.
(22) Alvarez, V. H.; Aznar, M. *Open Thermodyn. J.* **2008**, *2*, 25–38.
(23) Valderrama, J. O.; Reategui, A.; Sanga, W. W. *Ind. Eng. Chem. Res.* **2008**, *47*, 8416–8422.
(24) Cabaço, M. I.; Danten, Y.; Tassaing, T.; Longelin, S.; Besnard, M. *Chem. Phys. Lett.* **2005**, *413*, 258–262.
(25) Nelson, M. R.; Borkman, R. F. *J. Phys. Chem. A* **1998**, *102*, 7860–7863.
(26) Kazarian, S. G.; Vincent, M. F.; Bright, F. V.; Liotta, C. L.; Eckert, C. A. *J. Am. Chem. Soc.* **1996**, *118*, 1729–1736.
(27) Raveendran, P.; Wallen, S. L. *J. Am. Chem. Soc.* **2002**, *124*, 12590–12599.
(28) Sigma-Aldrich CBILS Chemical Synthesis: http://www.sigmaaldrich.com/Area_of_Interest/Chemistry/Chemical_Synthesis/Product_Highlights/CBILS.html.
(29) Freire, M. G.; Carvalho, P. J.; Fernandes, A. M.; Marrucho, I. M.; Queimada, A. J.; Coutinho, J. A. *J. Colloid Interface Sci.* **2007**, *314*, 621–630.
(30) Seddon, K. R.; Stark, A.; Torres, M. *Pure Appl. Chem.* **2000**, *72*, 2275–2287.
(31) Huddleston, J. G.; Visser, A. E.; Reichert, W. M.; Willauer, H. D.; Broker, G. A.; Rogers, R. D. *Green Chem.* **2001**, *3*, 156–164.
(32) Gardas, R. L.; Freire, M. G.; Carvalho, P. J.; Marrucho, I. M.; Fonseca, I. M. A.; Ferreira, A. G. M.; Coutinho, J. A. P. *J. Chem. Eng. Data* **2007**, *52*, 80–88.
(33) Blanchard, L.; Gu, Z.; Brennecke, J. *J. Phys. Chem. B* **2001**, *105*, 2437–2444.
(34) Fu, D.; Sun, X.; Pu, J.; Zhao, S. *J. Chem. Eng. Data* **2006**, *51*, 371–375.
(35) Vitu, S.; Jaubert, J. N.; Pauly, J.; Daridon, J. L.; Barth, D. *J. Supercrit. Fluids* **2008**, *44*, 155–163.
(36) Pauly, J.; Coutinho, J.; Daridon, J. L. *Fluid Phase Equilib.* **2007**, *255*, 193–199.
(37) Dias, A. M. A.; Carrier, H.; Daridon, J. L.; Pamies, J. C.; Vega, L. F.; Coutinho, J. A. P.; Marrucho, I. M. *Ind. Eng. Chem. Res.* **2006**, *45*, 2341–2350.
(38) Ventura, S. P. M.; Pauly, J.; Daridon, J. L.; Marrucho, I. M.; Dias, A. M. A.; Coutinho, J. A. P. *J. Chem. Eng. Data* **2007**, *52*, 1100–1102.
(39) Carvalho, P. J.; Álvarez, V. H.; Machado, J. J. B.; Pauly, J.; Daridon, J.; Marrucho, I. M.; Aznar, M.; Coutinho, J. A. P. *J. Supercrit. Fluids* **2009**, *48*, 99−107.
(40) Peng, D.; Robinson, D. B. *Ind. Eng. Chem. Fund.* **1976**, *15*, 59–64.
(41) Wong, D. S. H.; Sandler, S. I. *AIChE J.* **1992**, *38*, 671–680.
(42) Shin, E.; Lee, B.; Lim, J. S. *J. Supercrit. Fluids* **2008**, *45*, 282–292.
(43) Anthony, J.; Anderson, J.; Maginn, E.; Brennecke, J. *J. Phys. Chem. B* **2005**, *109*, 6366–6374.
(44) Letcher, T. M. *Developments and Applications in Solubility*; Royal Society of Chemistry: London, 2007.
(45) Cadena, C.; Anthony, J.; Shah, J.; Morrow, T.; Brennecke, J.; Maginn, E. *J. Am. Chem. Soc.* **2004**, *126*, 5300–5308.
(46) Kazarian, S. G.; Briscoe, B. J.; Welton, T. *Chem. Commun. (Cambridge)* **2000**, 2047–2048.
(47) Freire, M. G.; Carvalho, P. J.; Silva, A. M. S.; Santos, L. M. N. B. F.; Rebelo, L. P. N.; Marrucho, I. M.; Coutinho, J. A. P. *J. Chem. Phys. B* **2008**, *113*, 202–211.
(48) Diep, P.; Jordan, K.; Johnson, J.; Beckman, E. *J. Phys. Chem. A* **1998**, *102*, 2231–2236.
(49) Yonker, C.; Palmer, B. *J. Phys. Chem. A* **2001**, *105*, 308–314.
(50) Costa Gomes, M. F.; Padua, A. A. H. *J. Phys. Chem. B* **2003**, *107*, 14020–14024.

(51) Anderson, J. L.; Dixon, J. K.; Brennecke, J. F. *Acc. Chem. Res.* **2007**, *40*, 1208–1216.

(52) Anderson, J.; Ding, J.; Welton, T.; Armstrong, D. *J. Am. Chem. Soc.* **2002**, *124*, 14247–14254.

(53) Carvalho, P. J.; Alvarez, V. H.; Marrucho, I. M.; Aznar, M.; Coutinho, J. A. P. *Ind. Eng. Chem. Res.*, submitted for publication.

(54) Frisch, M. J.; Trucks, G. W.; Schlegel, H. B.; Scuseria, G. E.; Robb, M. A.; Cheeseman, J. R.; Montgomery, J. A., Jr.; Vreven, T.; Kudin, K. N.; Burant, J. C.; Millam, J. M.; Iyengar, S. S.; Tomasi, J.; Barone, V.; Mennucci, B.; Cossi, M.; Scalmani, G.; Rega, N.; Petersson, G. A.; Nakatsuji, H.; Hada, M.; Ehara, M.; Toyota, K.; Fukuda, R.; Hasegawa, J.; Ishida, M.; Nakajima, T.; Honda, Y.; Kitao, O.; Nakai, H.; Klene, M.; Li, X.; Knox, J. E.; Hratchian, H. P.; Cross, J. B.; Bakken, V.; Adamo, C.; Jaramillo, J.; Gomperts, R.; Stratmann, R. E.; Yazyev, O.; Austin, A. J.; Cammi, R.; Pomelli, C.; Ochterski, J. W.; Ayala, P. Y.; Morokuma, K.; Voth, G. A.; Salvador, P.; Dannenberg, J. J.; Zakrzewski, V. G.; Dapprich, S.; Daniels, A. D.; Strain, M. C.; Farkas, O.; Malick, D. K.; Rabuck, A. D.; Raghavachari, K.; Foresman, J. B.; Ortiz, J. V.; Cui, Q.; Baboul, A. G.; Clifford, S.; Cioslowski, J.; Stefanov, B. B.; Liu, G.; Liashenko, A.; Piskorz, P.; Komaromi, I.; Martin, R. L.; Fox, D. J.; Keith, T.; Al-Laham, M. A.; Peng, C. Y.; Nanayakkara, A.; Challacombe, M.; Gill, P. M. W.; Johnson, B.; Chen, W.; Wong, M. W.; Gonzalez, C.; Pople, J. A. *Gaussian 03*, Revision C.02; Gaussian: Wallingford, CT, 2004.

(55) Curtiss, L. A.; Raghavachari, K.; Redfern, P. C.; Rassolov, V.; Pople, J. A. *J. Chem. Phys.* **1998**, *109*, 7764–7776.

(56) Curtiss, L. A.; Redfern, P. C.; Raghavachari, K.; Rassolov, V.; Pople, J. A. *J. Chem. Phys.* **1999**, *110*, 4703–4709.

(57) Diadem Public 1.2. The DIPPR Information and Data Evaluation Manager, 2000.

JP901275B